


## PAPER

[View Article Online](#)  
[View Journal](#) | [View Issue](#)

Cite this: *Polym. Chem.*, 2025, **16**, 1238

# High performance polyurethanes derived from aromatic acetal-containing polyols enabling closed-loop recycling†

Patrick Schara,<sup>a</sup> Tankut Türel, <sup>a</sup> Anna Cristadoro,<sup>b</sup> Rint P. Sijbesma <sup>a</sup> and Željko Tomović \*<sup>a</sup>

Polyurethanes (PUs) are widely employed across diverse industries due to their versatility, durability, and mechanical strength. Enhancing their thermal and mechanical performance holds great potential for expanding their applicability and unlocking new market opportunities. This study addresses two key challenges: limited availability of aromatic polyols for high-performance PUs and their recycling issues. Incorporation of aromatic content in polyether polyols has traditionally been difficult using conventional methods. Herein, we developed three novel aromatic acetal-containing polyols through a green and solvent-free protocol *via* the polycondensation of aldehydes and diols, using acidic heterogeneous catalysts. Resulting polyols, with tailored aromatic content, significantly improved the mechanical strength of PUs, while maintaining low viscosity and easy processability. Besides that, PUs synthesized from these polyols exhibited excellent thermal stability and remarkable water resistance under neutral conditions. Additionally, these materials demonstrated efficient closed-loop recyclability through a novel transacetalization-based depolymerization under mild acidic conditions, yielding high purity monomers in good yields. This work introduces innovative aromatic polyacetal polyols, offering a sustainable approach to high-performance PUs. The approach also leverages the wide availability of diols and aldehydes, enabling the design of PUs with superior properties and closed-loop recycling.

Received 13th December 2024,

Accepted 29th January 2025

DOI: 10.1039/d4py01428f

[rsc.li/polymers](https://rsc.li/polymers)

## Introduction

Each year, approximately 400 million tons of plastics are produced globally, with polyurethanes (PUs) accounting for approximately 8% of the total due to their exceptional versatility.<sup>1</sup> This versatility makes PUs indispensable across a broad spectrum of applications, including rigid and flexible foams, elastomers, adhesives, and thermoplastics, all integral to modern life.<sup>2–4</sup> Although numerous grades of PU materials are already available, enhancing their physical properties can expand their applicability and open up new market opportunities.

Despite their widespread use, the end-of-life management of PU waste presents a significant and persistent challenge. The majority of PU waste is either landfilled or incinerated,

contributing to environmental pollution and the irreversible loss of valuable resources.<sup>5–7</sup> Current methods for processing PU waste predominantly rely on mechanical grinding, which involves grinding the waste into small particles and adding them as fillers in new PU product. Unfortunately, this approach produces materials with severely degraded properties, essentially downcycling the PU waste into low-value applications, such as carpet underlay and mats.<sup>8,9</sup>

To address these limitations, substantial research has been dedicated towards chemical recycling as a more sustainable alternative to mechanical recycling for PU materials. Common chemical recycling methods such as glycolysis,<sup>10–14</sup> hydrolysis,<sup>15–17</sup> aminolysis,<sup>18–21</sup> and acidolysis,<sup>22–24</sup> offer the potential to break down PUs into smaller components. However, these methods often require harsh reaction conditions, including high temperatures, pressures or excessive amounts of solvents and reactants. Additionally, they typically yield complex mixtures of polyols and oligomers that are cumbersome to isolate and purify to the same quality as virgin polyols, limiting their reuse in producing new PUs. These challenges have impeded the widespread commercial adoption of chemical recycling, leaving incineration and land-

<sup>a</sup>Department of Chemical Engineering and Chemistry, and Institute for Complex Molecular Systems, Eindhoven University of Technology, 5600 MB Eindhoven, The Netherlands. E-mail: [z.tomovic@tue.nl](mailto:z.tomovic@tue.nl)

<sup>b</sup>BASF Polyurethanes GmbH, Elastogranstraße 60, 49448 Lemförde, Germany

† Electronic supplementary information (ESI) available. See DOI: <https://doi.org/10.1039/d4py01428f>



filling as dominant waste management strategies for PU materials.

To enhance the recyclability of PU materials, significant research efforts have focused on incorporating cleavable bonds into PU structures, particularly within the polyol component. Acetal functionalities have emerged as a promising candidate due to their stability under neutral or basic conditions and selective hydrolysis under acidic environments.<sup>25–29</sup> In our recent works, we developed acetal polyols *via* solvent-free synthesis using heterogeneous catalysts. These polyols were then utilized for the preparation of PU materials amenable to closed loop recycling.<sup>30</sup>

Beyond improving recyclability, another key area of PU research is the incorporation of aromatic groups into the polyol structures, which can significantly enhance mechanical strength, thermal stability, and fire retardance.<sup>31–37</sup> Typically, commercial polyether polyols are synthesized through the ring-opening of either propylene oxide or ethylene oxide, which does not allow for the incorporation of significant aromatic content. Additionally, the use of aromatic polyols presents its own challenge: increasing the aromatic content often raises the melting points and viscosities of polyols, complicating the bulk synthesis of PUs, which significantly limits their industrial applicability. For example, polyols used for the synthesis of PU cast elastomers are frequently processed at temperatures ranging from 45 to 75 °C, while for thermoplastic PU typically at processing temperature of ~80 °C.<sup>4</sup> Therefore, ensuring that polyols are processable within this temperature range is crucial for their successful application in polyurethane production. Consequently, polyether polyols with high aromatic content remain scarce in the literature, with most examples featuring only limited aromatic incorporation.

In this work, improvements in both the mechanical performance and recyclability of PU materials are addressed. Specifically, we developed a green protocol for the synthesis of an array of acetal-containing polyols with aromatic motifs *via* the polycondensation of diols and aldehydes, utilizing either aromatic aldehydes or aromatic diols (Fig. 1A). This strategy enabled the design of highly aromatic polyols with a broad range of properties. The resulting PU materials not only exhibited superior mechanical properties to the conventional PUs but also demonstrated efficient closed-loop recyclability (Fig. 1B). The hydrolysis of these acetal-containing PUs allowed the recovery of the original monomers with high yields and purity. Furthermore, monomer recovery process was enhanced through transacetalization, utilizing environmentally benign alcohols and acids. Notably, this work marks the first use of transacetalization method for the depolymerization of acetal containing polymer materials. This approach enables efficient recycling under milder conditions, avoiding the harsh conditions and long reaction times typically required by conventional hydrolysis methods. Furthermore, this work highlights the potential of acetal chemistry to advance the development of sustainable, recyclable polyurethanes with superior mechanical performance, addressing key challenges in both recyclability and material properties.

## Results and discussion

### Synthesis and characterization of aromatic acetal-containing polyols

Advancing previous synthetic methods for aliphatic acetal polyols (APs) described in our previous work,<sup>30</sup> herein, we developed a green protocol for the synthesis of novel aromatic APs. Using this new approach, three novel aromatic polyols, **AP1–AP3**, were prepared, with aromatic contents ranging from 11 to 35 wt%. **AP1** and **AP2** were synthesized *via* the polycondensation of paraformaldehyde with 1,6-hexanediol (H16) and 1,4-bis(2-hydroxyethoxy)benzene (HEB) in varying ratios, utilizing a commercial silica-alumina heterogeneous acid catalyst, Siral 70 (see ESI for more details, Scheme S1–S3†). Specifically, **AP1** was produced with a ratio of 1 : 0.2, while **AP2** utilized a ratio of 1 : 0.8. **AP2** was optimized to maximize HEB content without increasing the melting point and viscosity of the polyol beyond practical limits for polyurethane applications. An alternative method for incorporating aromatic units into APs as a side group involved the condensation of aromatic aldehydes with diols utilizing a commercial copper-based metal organic framework heterogeneous acid catalyst, C300. **AP3**, synthesized through the condensation of benzaldehyde and H16 using the same heterogeneous acid catalyst, achieved the highest aromatic content among the polyols at 35 wt%, as confirmed by <sup>1</sup>H-NMR spectra (Fig. S1–S3†). After filtration of the reaction mixture to remove the heterogeneous acid catalyst, the resulting polyols were transparent, colorless, and had an acid value below the detection limit (0.08 mg KOH g<sup>−1</sup>). Table 1 provides a comprehensive summary of the prepared APs, including their structures and properties. The purity and structure of **AP1–3** were confirmed with <sup>1</sup>H-NMR and matrix-assisted laser desorption ionization time-of-flight mass spectrometry (MALDI-TOF-MS) (Fig. 2 and Fig. S1–S3†). The <sup>1</sup>H-NMR spectra (Fig. 2) displayed characteristic acetal proton signals for each polyol. **AP1** and **AP2** showed three distinct acetal signals at 4.66, 4.75, and 4.85 ppm, corresponding to the different acetal groups within the copolymer structure of H16 and HEB repeating units (Fig. S4†). For both **AP1** and **AP2** the monomer ratio matches the feed ratio closely. Additionally, the relative intensities of the acetal signals indicate that HEB incorporation is statistical, with acetals bridging two HEB units (4.85 ppm) being only a minor product in both **AP1** and **AP2**. These findings confirm the statistical incorporation of HEB throughout the polyols in proportions consistent with the monomer feed ratios. As expected, **AP3** displayed a single acetal proton signal, with no detectable impurities. MALDI-TOF-MS analysis was employed to further validate the polymer structures. The mass spectra for **AP1** and **AP2** showed a spacing of 130.10 and 210.08 Da between the peaks, corresponding precisely to the mass values of the H16 and HEB repeating units, respectively. The absolute peak values also matched the theoretical molar mass of the polymer chains with varying numbers of repeating units, with an additional sodium cation (*e.g.*, [M + Na]<sup>+</sup> for **AP1**, the peak at 1131.75 Da corresponds to a polymer chain with seven H16 units and one



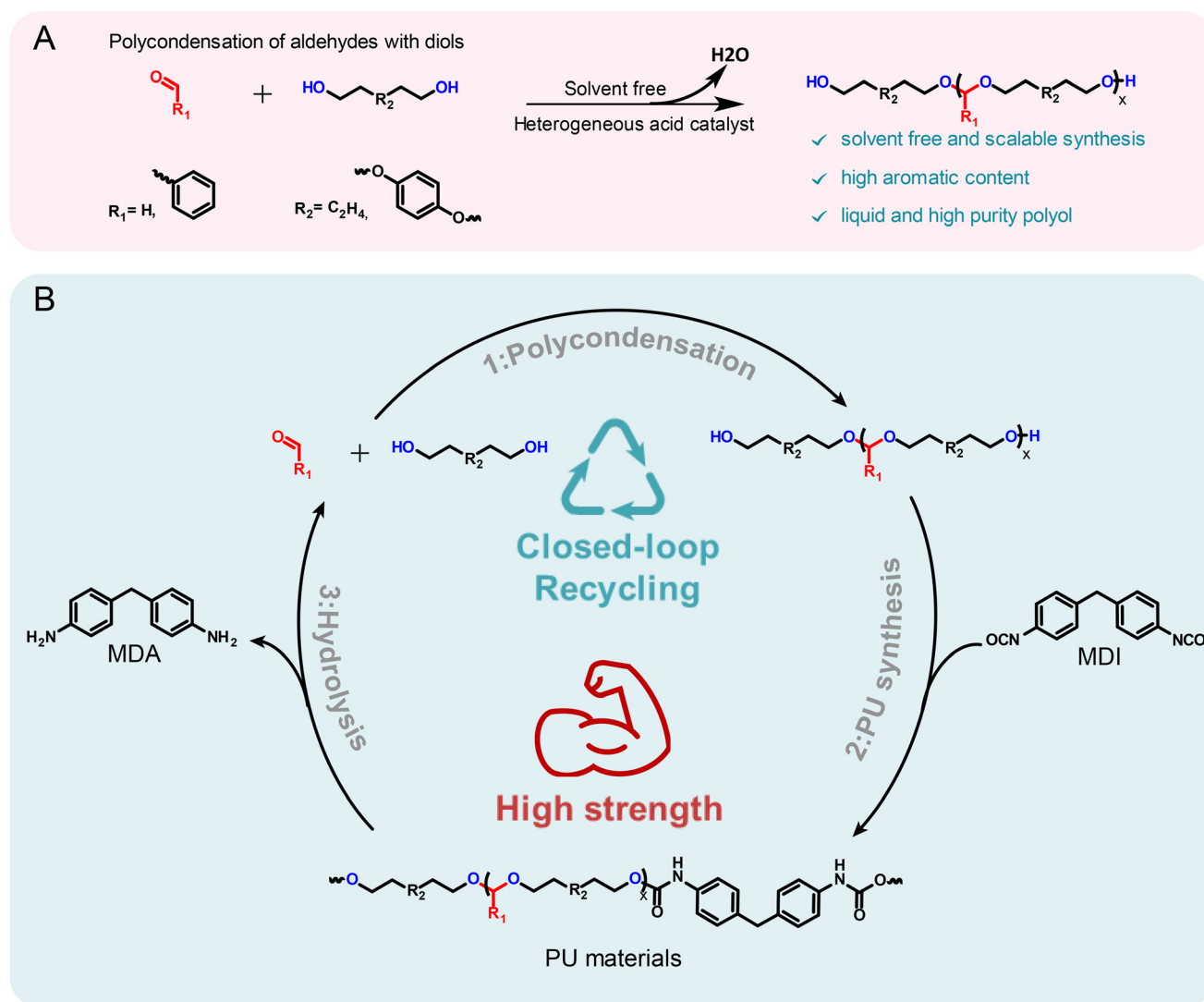
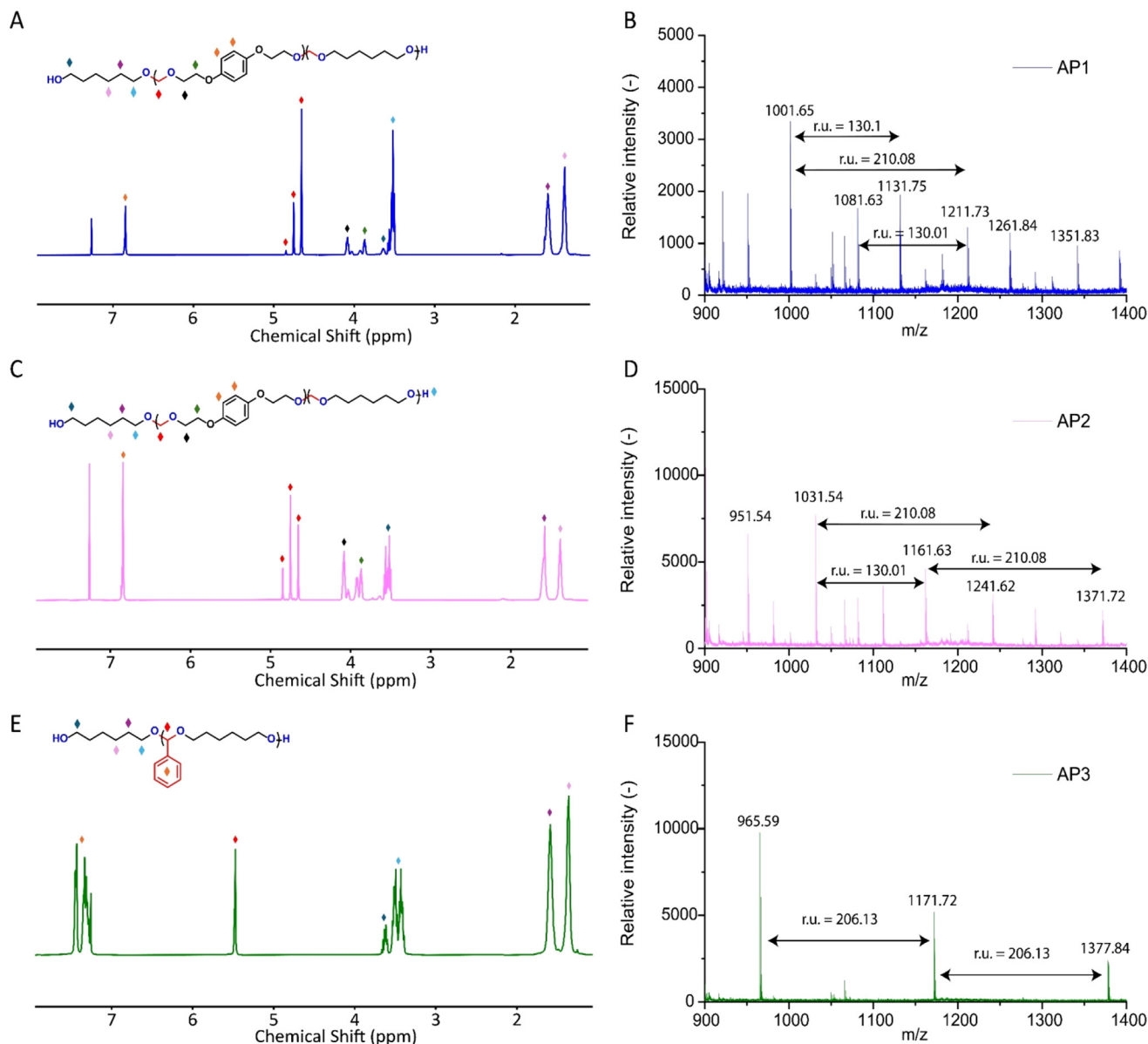


**Fig. 1** Synthesis and utilization of aromatic acetal-containing polyol in high performance closed-loop recyclable polyurethanes. (A) Synthetic route for aromatic acetal-containing polyols via the condensation of diols with aldehydes, facilitated by a heterogeneous acid catalyst. (B) Proposed closed-loop recycling scheme of acetal-containing high-performance PU materials back into original monomers.

**Table 1** The structures and the properties of APs studied in this work

Polyol name	Polyol structure	Aromatic content (wt%)	Viscosity at 65 °C (mPa s)	$M_n$ based on $^1\text{H-NMR}$ (g mol $^{-1}$ )	OH# (mg KOH g $^{-1}$ )
AP 1		11	97	1370	77
AP 2		23	250	1400	81
AP 3		35	330	1430	84





Differential scanning calorimetry (DSC) was employed to investigate the thermal properties of the polyols (Fig. S7†). Both **AP1** and **AP2** exhibited distinct crystallization and melting behavior. **AP1** showed a melting point around 10 °C, while **AP2** displayed a broad melting peak between 30 and 70 °C, indicative of its higher aromatic content as compared with **AP1**. Additionally, the glass transition temperatures ( $T_g$ ) of **AP1**, **AP2**, and **AP3** were found to be −70 °C, −47 °C, and −43 °C, respectively, reflecting the increasing rigidity of the polyols with higher aromatic content.

The hydrolytic stability of **AP1–AP3** was investigated in an acidic water/THF mixture at 50 °C using *p*-toluenesulfonic acid as an acid catalyst utilizing *in situ*  $^1\text{H}$ -NMR spectroscopy (Fig. S8–S10†). The obtained  $^1\text{H}$ -NMR spectra were used to calculate the percentage of remaining acetal bonds over time (Fig. 3). **AP1** and **AP2** demonstrated exceptional hydrolytic stability, with no detectable hydrolysis or aldehyde formation after 15 hours, indicating that the acetal bonds in these polyols remain intact under acidic conditions. This result underscores the robust nature of these polyols, particularly **AP1** and **AP2**, in environments where hydrolytic degradation is a concern. In contrast, **AP3** underwent rapid hydrolysis under acidic conditions, with complete loss of acetals within 2 hours, accompanied by the formation of the benzaldehyde. Notably, the acetal concentration in **AP3** approached zero, rather than reaching an equilibrium with the free aldehyde present in the solution, which is in contrast to the previous observations in studies involving acetals derived from acetaldehyde.<sup>30</sup> The significant difference between the hydrolytic susceptibility of the benzaldehyde based polyol **AP3** compared to the formaldehyde based **AP1** and **AP2** are consistent with previous literature. Accordingly, the hydrolytic stability of acetals under acidic conditions is influenced by the substituents on the acetal bridge. Acetals with a methylene bridge (*i.e.*, **AP1** and **AP2**) exhibit sig-

nificantly higher stability compared to those with additional substituents such as **AP3**. This is due to the stabilizing effect of the side groups on the cationic hydrolysis intermediate.<sup>38</sup>

### Synthesis and characterization of acetal polyol containing PU materials

Acetal containing PU materials were synthesized by reacting **AP1–3** with 4,4'-methylene diphenyl diisocyanate (4,4'-MDI) and H16, maintaining an NCO-to-hydroxyl ratio of 1.01 : 1 in all formulations. The successful formation of urethane linkages was confirmed by FTIR, as indicated by the appearance of a carbonyl (C=O) stretch at 1700  $\text{cm}^{-1}$  and the disappearance of the isocyanate (N=C=O) stretching band at 2260  $\text{cm}^{-1}$  (Fig. S11†). The carbonyl region around 1700  $\text{cm}^{-1}$  consists of two distinct stretching peaks: the non-hydrogen bonded C=O at 1730  $\text{cm}^{-1}$  and the hydrogen-bonded C=O at 1700  $\text{cm}^{-1}$ , which is typical for phase-separated polyurethanes.<sup>39,40</sup> Since hydrogen bonding predominantly occurs in the hard phase, the degree of phase separation between soft and hard phases can be inferred by comparing the intensity of these two carbonyl signals. The ratio of the hydrogen-bonded to non-hydrogen-bonded carbonyl groups was calculated by comparing the areas under the peaks (Fig. S12†). Among the PUs, **PU AP3** exhibited the highest ratio of 2.6, suggesting the greatest degree of phase separation. This was followed by **PU AP1** (2.1), and **PU AP2** (1.4). These results suggest that the presence of HEB increases interphase mixing, leading to reduced hydrogen bonding compared to **PU AP3**. GPC measurements were performed to determine the molar mass of the PUs, which showed weight-average molar mass ( $M_w$ ) exceeding 100  $\text{kg mol}^{-1}$  for all samples (Fig. S13†). **PU AP1** and **PU AP3** showed similar dispersities, with values of 2.8 and 2.6, respectively. **PU AP2** possessing a higher molecular weight, exceeded the exclusion limit of the GPC column, leading to an high apparent molar mass shoulder at the exclusion limit. Thermal properties of the acetal-containing PU materials were evaluated using thermogravimetric analysis (TGA), and DSC. TGA demonstrated good thermal stability for all three PU materials, with initial degradation temperatures ( $T_{d5\%}$ ) around 310 °C, which could be correlated with the degradation of the urethane bonds (Fig. 4A).<sup>39</sup> At higher temperatures, **PU AP3** degraded almost completely by 400 °C, leaving less than 10 wt% of material, while **PU AP1** and **PU AP2** retained about 60 wt% at this temperature. **PU AP1** and **PU AP2** showed two distinct temperatures of maximum degradation rate ( $T_{d,\text{max}}$ ) at approximately 340 °C and 430 °C, with the latter attributed to the degradation of the polyol soft phase (Fig. 4A).<sup>39</sup> The differences in thermal characteristics can be attributed to the lower thermal stability of the aromatic acetal groups present in **PU AP3** compared to the formaldehyde-based acetal groups in **PU AP1** and **PU AP2**. DSC analysis revealed a soft phase  $T_g$  of −36 °C, 1 °C, and −18 °C for **PU AP1**, **PU AP2**, and **PU AP3**, respectively (Fig. 4B). Notably, **PU AP2** exhibited the highest  $T_g$ , despite its constituent polyol (**AP2**) having a glass transition temperature comparable to that of **AP3** (~−45 °C). The substantial increase in the  $T_g$  of **PU AP2**

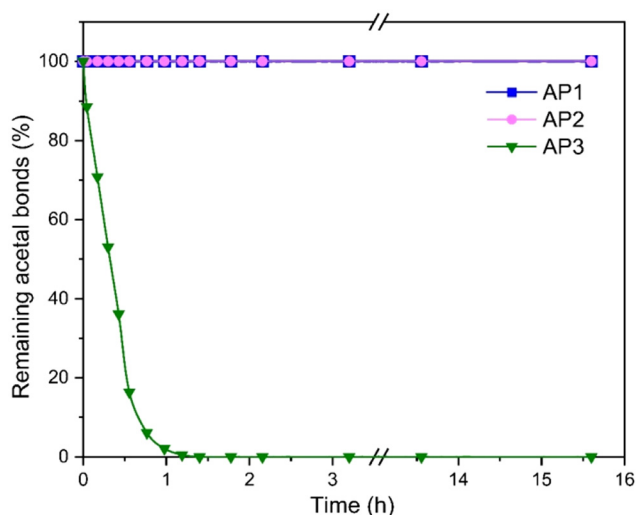
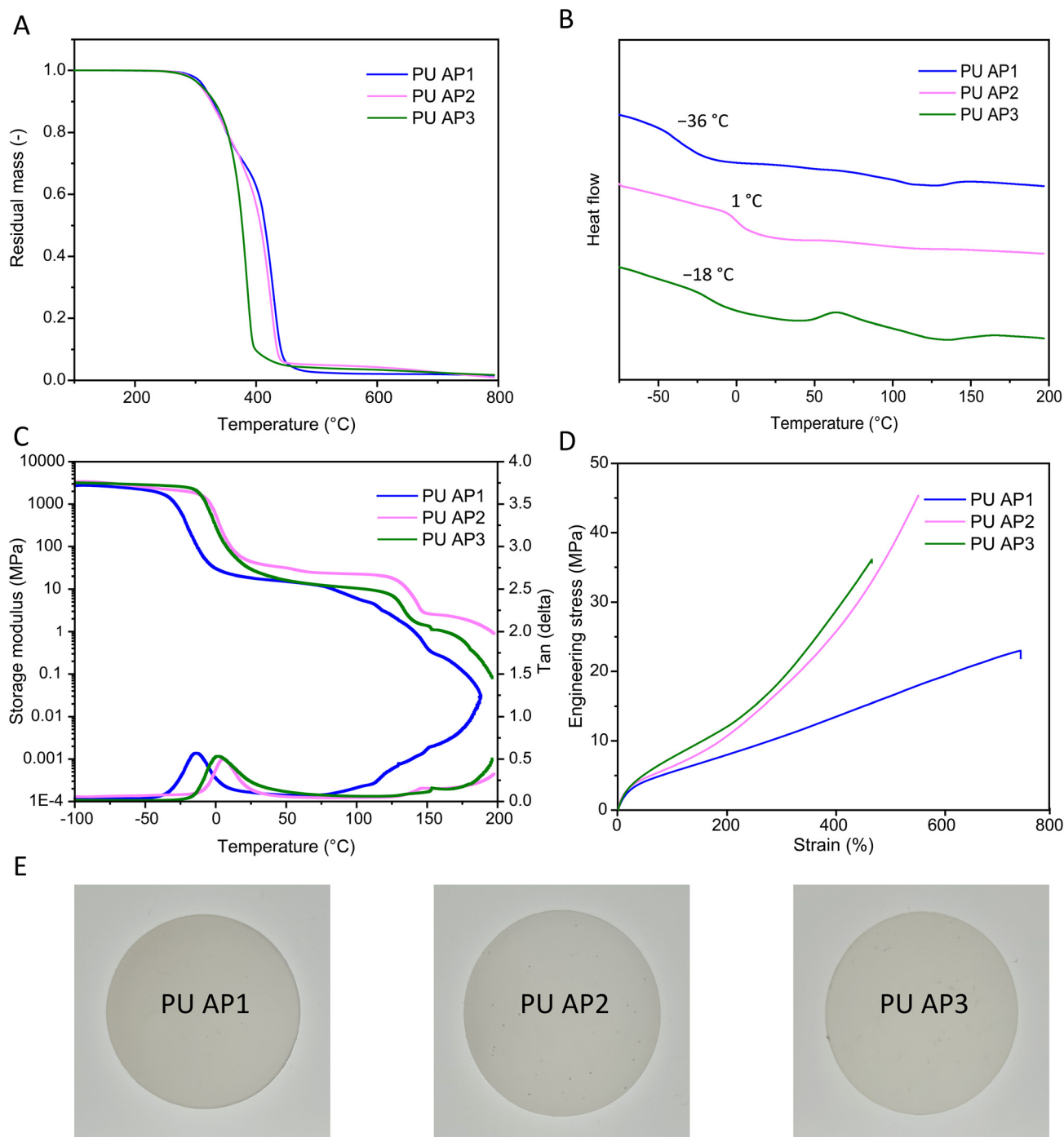


Fig. 3 Degree of hydrolysis of **AP1–AP3** under acidic conditions measured by  $^1\text{H}$ -NMR over a period of 16 h (200 mg polyol in 1 ml THF- $d_8$  with 0.2 g of a 20 mM *p*-toluenesulfonic acid aqueous solution).







**Fig. 4** Thermo-mechanical properties of the acetal-containing PUs. (A) TGA (B) DSC, (C) DMA curves, (D) stress–strain, (E) photographs of the bulk cast material.

compared to the more modest increase observed in the  $T_g$  of **PU AP3** relative to their respective acetals, could be explained by the mixing of the hard phase in the soft phase.<sup>41</sup> The degree of phase separation, could be predicted based on the differences in  $T_g$  of the PUs with respect to their constituent acetals polyols. Accordingly, the degree of phase separation was lowest in **PU AP2**, followed by **PU AP1** and highest in **PU AP3**, aligning with the findings from the FTIR analysis.

Dynamic mechanical analysis (DMA) provided further insights into the thermomechanical behavior.  $T_g$  values, derived from the maxima of  $\tan(\delta)$  curves, were  $-14\text{ }^{\circ}\text{C}$ ,  $2\text{ }^{\circ}\text{C}$ , and  $7\text{ }^{\circ}\text{C}$  for **PU AP1**, **PU AP2**, and **PU AP3**, respectively, which followed a similar trend to those observed in DSC. Melting points were indicated by a drop in storage modulus around  $130\text{ }^{\circ}\text{C}$ . Notably, the modulus did not immediately drop to zero, indicating solid-like behavior persisted up to  $200\text{ }^{\circ}\text{C}$ ,



highlighting the mechanical robustness of the materials at elevated temperatures (Fig. 4C).

Tensile testing revealed excellent mechanical properties across all PU samples. **PU AP1** showed the highest elongation of  $663 \pm 22\%$  and the lowest stress at break of  $23 \pm 1$  MPa, making it the most flexible material among the samples. In contrast, **PU AP2** and **PU AP3**, having higher aromatic content, exhibited lower flexibility. **PU AP2** stood out for its exceptional mechanical performance, including high elongation at break ( $560 \pm 38\%$ ), the highest stress at break ( $47 \pm 8$  MPa), and Young's modulus ( $37 \pm 2$  MPa), resulting in a remarkable toughness exceeding  $100 \text{ MJ m}^{-3}$ , equal to or even surpassing high-performance polyurethanes (Table 2 and Fig. 4D).<sup>32,42,43</sup>

To assess the hydrolytic stability of the PU material, tensile test specimens of **PU AP2** were fully submerged in distilled water at  $70^\circ\text{C}$  for 48 hours. After drying under vacuum at  $70^\circ\text{C}$  for 5 hours, the mechanical properties of the samples remained nearly identical to those of the original, non-exposed specimens. Additionally, the exposed samples showed no visible changes compared to the original films, and the GPC curve of the exposed sample was nearly identical to that of the original, further confirming excellent hydrolytic stability (Fig. 5 and Table 3)

### Closed-loop recycling of PU materials

To explore the potential for closed-loop recycling of **PU AP1–3**, we investigated their hydrolysis under acidic conditions. This process allows the acetal-containing PUs to be chemically recycled back into their original components (*i.e.*, diols, aldehydes), and a urethane-rich hard phase, which can be easily separated through filtration and distillation. The isolated hard phase was further depolymerized into diols and 4,4'-Methylenedianiline (MDA), the precursor of 4,4'-MDI (Fig. 6A).

Significant differences in hydrolytic stability under acidic conditions were observed among the PU samples, particularly between **PU AP1–2** and **PU AP3**, in accordance with the results shown in Fig. 3. **PU AP3** was quickly hydrolyzed under relatively mild conditions, whereas **PU AP1** and **PU AP2** exhibited much greater hydrolytic stability under acidic conditions. Both  $0.3 \text{ M HCl}$  and  $1 \text{ M H}_3\text{PO}_4$  were effective in hydrolyzing the acetal bonds fully in **PU AP3**, producing free benzaldehyde within 24 hours, as confirmed by  $^1\text{H-NMR}$  spectra (Fig. S14 and S15†). In contrast, attempts to recycle **PU AP2** were hampered by its higher acetal stability and low swelling in water, resulting in significantly slower hydrolysis rates. Even treatment with  $2 \text{ M}$  and  $4 \text{ M HCl}$  solutions yielded partial hydrolysis, leaving a considerable amount of acetals intact.

**Table 2** Thermo-mechanical properties of the acetal-containing PU materials

PU materials	$T_{d5\%}$ ( $^\circ\text{C}$ )	$T_g$ (DSC), ( $^\circ\text{C}$ )	$T_g$ (DMA), ( $^\circ\text{C}$ )	Young's modulus (MPa)	Stress at break (MPa)	Elongation (%)	Toughness ( $\text{MJ m}^{-3}$ )
<b>PU AP1</b>	313	−36	−14	$24 \pm 2$	$23 \pm 1$	$663 \pm 22$	$96 \pm 7$
<b>PU AP2</b>	308	1	6	$37 \pm 2$	$47 \pm 8$	$560 \pm 38$	$105 \pm 21$
<b>PU AP3</b>	310	−18	2	$28 \pm 3$	$37 \pm 1$	$470 \pm 4$	$75 \pm 3$

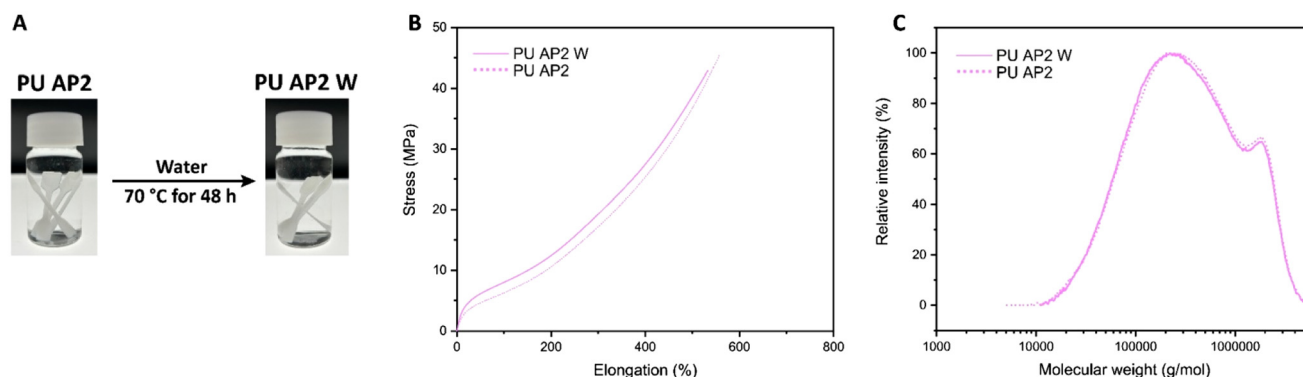


**Fig. 5** (A) Photographs of **PU AP2** before and after water exposure, (B) Stress–strain curves, and (C) GPC traces of the specimens.

**Table 3** Mechanical properties of the acetal-containing PU materials before and after water exposure

PU materials	Elongation (%)	Stress at break (MPa)	Young's modulus (MPa)	Toughness ( $\text{MJ m}^{-3}$ )	$M_n$ based on GPC ( $\text{Kg mol}^{-1}$ )
<b>PU AP2</b>	$560 \pm 38$	$47 \pm 8$	$37 \pm 2$	$105 \pm 21$	147
<b>PU AP2 W</b>	$529 \pm 7$	$45 \pm 1$	$45 \pm 2$	$103 \pm 3$	147



To accelerate hydrolysis and reduce the required acidity, we investigated aqueous acidic solutions in the presence of several green organic solvents such as 2-methyltetrahydrofuran (Me-THF), acetone, and ethanol. Among these, ethanol demonstrated the highest efficacy, as confirmed by  $^1\text{H-NMR}$  analysis (Fig. S16†). The effectiveness of ethanol is attributed to its role in the trans-acetalization reaction, wherein it inserts into the acetal linkages of the polyol chain, producing soluble oligomers which are more readily hydrolyzed (Scheme S4†). This results in a synergistic depolymerization process that simultaneously utilizes hydrolysis and trans-acetalization path-

ways. The depolymerization of acetal containing polymers using this strategy has never been demonstrated. This process generates highly volatile aldehydes or acetals, which can be easily recovered *via* condensation from the gas stream.<sup>44,45</sup> Such a method would allow for the efficient recovery of monomers in industrial processes.

In the depolymerization studies, both **PU AP2** and **PU AP3** were treated with an ethanol-2 M  $\text{H}_3\text{PO}_4(\text{aq})$  (9 : 1) mixture at reflux temperature. For instance, **PU AP3** (44 g in centimeter-sized chunks) was fully depolymerized within 5 hours. Upon completion of the hydrolysis, water was added to induce the

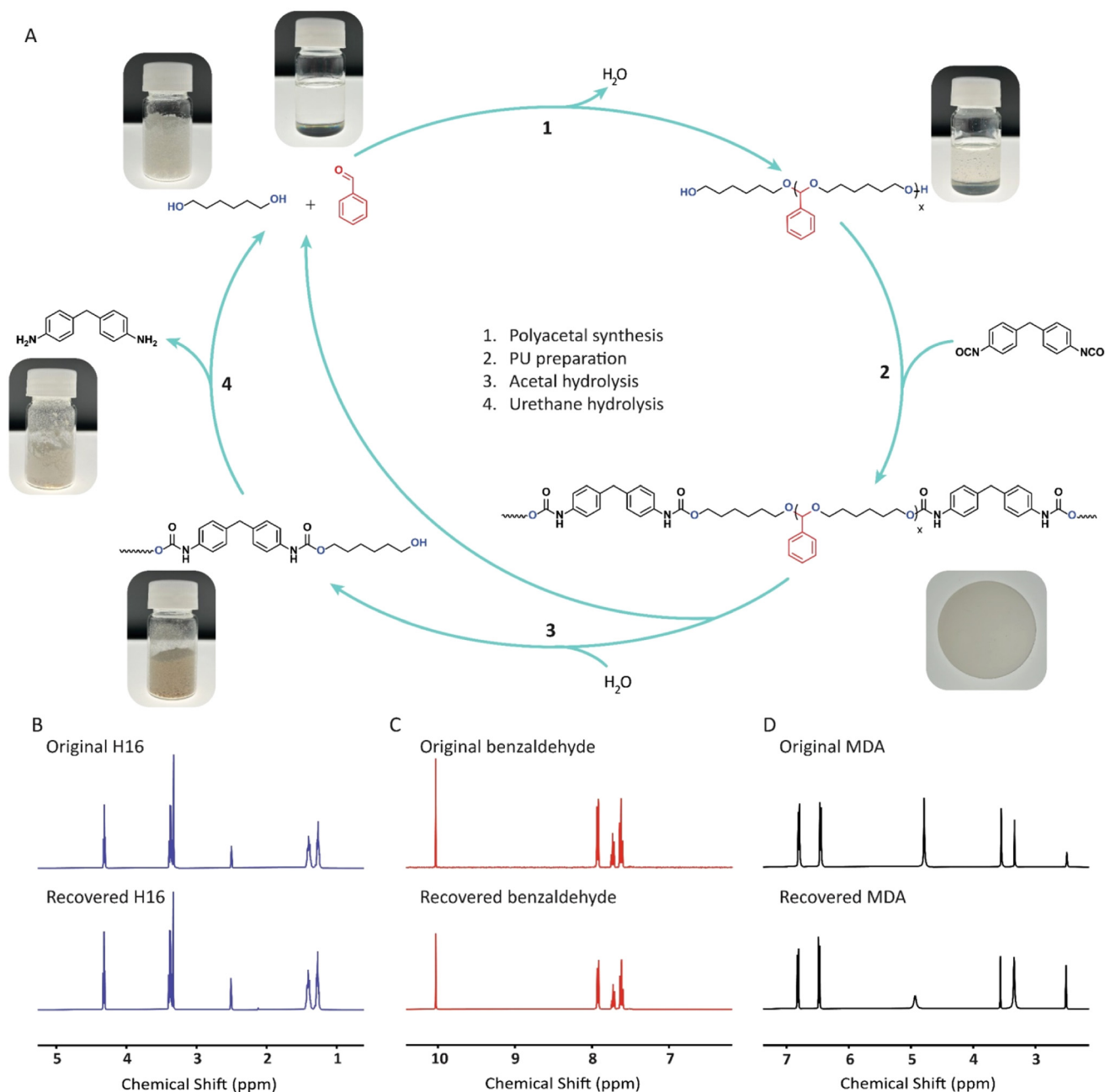


**Fig. 6** (A) Synthesis and chemical recycling of **PU AP3**. (B, C and D)  $^1\text{H-NMR}$  spectra (400 MHz,  $\text{DMSO-d}_6$ ) of the original (top) and recovered (bottom) monomers, H16 (B), Benzaldehyde (C), and MDA (D).





precipitation of the hard phase, which was then removed *via* filtration. The resulting filtrate, containing H16 and benzaldehyde, was extracted with ethyl acetate, to isolate both building blocks, followed by vacuum distillation of each component. Accordingly, benzaldehyde was isolated with a yield of 57%. On the other hand, the precipitated hard phase was further subjected to base-catalyzed hydrolysis with 8 wt% TBD and 16 wt% water at 120 °C. After 36 hours, H16 was recovered from the water-soluble phase by vacuum distillation and combined with the portion obtained from the first hydrolysis step, giving a total recovery yield of 90%. Meanwhile, MDA was recovered from the water-insoluble residue through vacuum distillation and further purified *via* recrystallization from water, achieving a final yield of 68%. All recovered monomers exhibited high purity, as illustrated in Fig. 6 and Fig. S17–S22.† **PU AP2** (20 g) was also depolymerized under the same conditions to achieve monomer recovery yields of 69%, 79% and 74% for HEB, H16 and MDA, respectively. The corresponding <sup>1</sup>H-NMR spectra of the recovered monomers are shown in Fig. S23–S27.† The successful depolymerization of both **PU AP2** and **PU AP3** *via* ethanol-assisted trans-acetalization demonstrates that even hydrolytically stable acetal-containing PUs can be effectively closed-loop recycled using green acids and solvents under mild conditions.

## Conclusion

Herein, we successfully developed three aromatic acetal-containing polyols through the polycondensation of aldehydes and diols using acidic heterogeneous catalysts. The aromatic content of these polyols could be modulated as high as 35 wt% while still maintaining an easily processable, low viscosity liquid polyol. Furthermore, these polyols exhibited a wide range of properties, including varying degrees of hydrolytic stability under acidic conditions. When utilized to produce PU materials, the resulting materials demonstrated exceptional mechanical and thermal properties, highlighting their potential in high-performance applications. For example, **PU AP2** exhibited a unique combination of mechanical properties, with a high elongation at break ( $560 \pm 38\%$ ), the highest stress at break ( $47 \pm 8$  MPa), and a high Young's modulus ( $37 \pm 2$  MPa). Such characteristics contributed to a toughness of over  $100 \text{ MJ m}^{-3}$ , surpassing the performance of many conventional polyurethanes. These results underscore the versatility of polycondensation of aldehydes and diols as a method for designing acetal-containing polyols with tailored properties, such as high mechanical performance. A key novel advancement of this work is the efficient depolymerization of the synthesized PUs using ethanol, which facilitates transacetalization of the acetal units utilizing phosphoric acid, thus enabling closed-loop recycling under milder conditions compared to conventional hydrolysis methods. The urethane-rich hard phase remaining after this process was also successfully depolymerized into well-defined monomers. Specifically, **PU AP3** was depolymerized into 1,6-hexanediol (H16) and benz-

aldehyde, while the hard phase yielded 4,4'-methylenedianiline (MDA) and H16, with a final yield of 90% for H16, 57% for benzaldehyde, and 68% for MDA. Similarly, **PU AP2** was hydrolyzed into 1,6-hexanediol, 1,4-bis(2-hydroxyethoxy)benzene, and MDA, achieving yields of 69%, 79%, and 74%, respectively. Given the broad availability and diversity of diols and aldehydes, this synthetic approach opens the door for the design of acetal-containing polyols with customized features such as varying polarity, crystallinity, aromatic content, or biobased content. Consequently, this work paves the way for the development of sustainable polyurethane materials with novel properties, advancing the concept of closed-loop recycling in the field of high-performance plastics.

## Data availability

The authors confirm that the data supporting the findings of this study are available within the article and its ESI.† The data are available from the corresponding author upon reasonable request.

## Conflicts of interest

There are no conflicts to declare.

## Acknowledgements

The authors would like to thank Xianwen Lou (TU Eindhoven) for MALDI-TOF-MS measurements, and SASOL (Germany) for providing the Siral catalysts. The authors acknowledge financial support from BASF Polyurethanes GmbH (Germany) and the Dutch Ministry of Economic Affairs and Climate Policy (TKI project CHEMIE.PGT.2020.022).

## References

- 1 Plastics Europe, Plastics-the Facts 2021, (accessed August 9, 2023).
- 2 H.-W. Engels, H.-G. Pirkel, R. Albers, R. W. Albach, J. Krause, A. Hoffmann, H. Casselmann and J. Dormish, *Angew. Chem., Int. Ed.*, 2013, **52**, 9422–9441.
- 3 B. Eling, Ž. Tomović and V. Schädler, *Macromol. Chem. Phys.*, 2020, **221**, 2000114.
- 4 D. Randall and S. Lee, *The polyurethanes book*, Wiley, 2003.
- 5 R. Geyer, J. R. Jambeck and K. L. Law, *Sci. Adv.*, 2017, **3**, e1700782.
- 6 B. Liu, Z. Westman, K. Richardson, D. Lim, A. L. Stottlemeyer, T. Farmer, P. Gillis, V. Vlcek, P. Christopher and M. M. Abu-Omar, *ACS Sustainable Chem. Eng.*, 2023, **11**, 6114–6128.
- 7 C. Liang, U. R. Gracida-Alvarez, E. T. Gallant, P. A. Gillis, Y. A. Marques, G. P. Abramo, T. R. Hawkins and J. B. Dunn, *Environ. Sci. Technol.*, 2021, **55**, 14215–14224.



- 8 D. Simón, A. M. Borreguero, A. de Lucas and J. F. Rodríguez, *Waste Manage.*, 2018, **76**, 147–171.
- 9 J. Banik, D. Chakraborty, M. Rizwan, A. H. Shaik and M. R. Chandan, *Waste Manage. Res.*, 2023, **41**, 1063–1080.
- 10 T. Vanbergen, I. Verlent, J. De Geeter, B. Haelterman, L. Claes and D. De Vos, *ChemSusChem*, 2020, **13**, 3835–3843.
- 11 P. Jutrzenka Trzebiatowska, H. Beneš and J. Datta, *React. Funct. Polym.*, 2019, **139**, 25–33.
- 12 D. Simón, A. M. Borreguero, A. de Lucas and J. F. Rodríguez, *Polym. Degrad. Stab.*, 2015, **116**, 23–35.
- 13 R. Donadini, C. Boaretti, A. Lorenzetti, M. Roso, D. Penzo, E. Dal Lago and M. Modesti, *ACS Omega*, 2023, **8**, 4655–4666.
- 14 M. B. Johansen, B. S. Donslund, E. Larsen, M. B. Olsen, J. A. L. Pedersen, M. Boye, J. K. C. Smedsgård, R. Heck, S. K. Kristensen and T. Skrydstrup, *ACS Sustainable Chem. Eng.*, 2023, **11**, 10737–10745.
- 15 S. Zamani, J.-P. Lange, S. R. A. Kersten and M. P. Ruiz, *Polymers*, 2022, **14**, 4869.
- 16 Y. Branson, S. Sötl, C. Buchmann, R. Wei, L. Schaffert, C. P. S. Badenhorst, L. Reisky, G. Jäger and U. T. Bornscheuer, *Angew. Chem., Int. Ed.*, 2023, **62**, e202216220.
- 17 S. Motokuchō, Y. Nakayama, H. Morikawa and H. Nakatani, *J. Appl. Polym. Sci.*, 2018, **135**, 45897.
- 18 I. Olazabal, A. González, S. Vallejos, I. Rivilla, C. Jehanno and H. Sardon, *ACS Sustainable Chem. Eng.*, 2023, **11**, 332–342.
- 19 M. Grdadolnik, B. Zdobc, A. Drinčić, O. C. Onder, P. Utroša, S. G. Ramos, E. D. Ramos, D. Pahovnik and E. Žagar, *ACS Sustainable Chem. Eng.*, 2023, **11**, 10864–10873.
- 20 S. Bhandari and P. Gupta, in *Recycling of Polyurethane Foams*, ed. S. Thomas, A. V. Rane, K. Kanny, A. Vayyaprontavida Kaliyathan and M. G. Thomas, William Andrew Publishing, 2018, pp. 77–87.
- 21 H. Watando, S. Saya, T. Fukaya, S. Fujieda and M. Yamamoto, *Polym. Degrad. Stab.*, 2006, **91**, 3354–3359.
- 22 M. Grdadolnik, A. Drinčić, A. Oreški, O. C. Onder, P. Utroša, D. Pahovnik and E. Žagar, *ACS Sustainable Chem. Eng.*, 2022, **10**, 1323–1332.
- 23 H. He, H. Su, H. Yu, K. Du, F. Yang, Y. Zhu, M. Ma, Y. Shi, X. Zhang, S. Chen and X. Wang, *ACS Sustainable Chem. Eng.*, 2023, **11**, 5515–5523.
- 24 Z. Westman, B. Liu, K. Richardson, M. Davis, D. Lim, A. L. Stottlemeyer, C. S. Letko, N. Hooshyar, V. Vlcek, P. Christopher and M. M. Abu-Omar, *JACS Au*, 2024, **4**(8), 3194–3204.
- 25 M. Ionescu, S. Sinharoy and Z. S. Petrović, *J. Polym. Environ.*, 2009, **17**, 123.
- 26 A. Iinuma, T. Hashimoto, M. Urushisaki and T. Sakaguchi, *J. Appl. Polym. Sci.*, 2016, **133**, 44088.
- 27 P. Schara, A. M. Cristadoro, R. P. Sijbesma and Ž. Tomović, *Macromolecules*, 2023, **56**, 8866–8877.
- 28 T. Türel, Ö. Dağlar, C. Pantazidis and Ž. Tomović, *RSC Sustainability*, 2024, **2**(11), 3311–3319.
- 29 T. Türel and Ž. Tomović, *ACS Sustainable Chem. Eng.*, 2023, **11**, 8308–8316.
- 30 P. Schara, A. Cristadoro, R. P. Sijbesma and Ž. Tomović, *ChemSusChem*, 2024, e202401595.
- 31 N. Mahmood, Z. Yuan, J. Schmidt and C. (Charles) Xu, *Renewable Sustainable Energy Rev.*, 2016, **60**, 317–329.
- 32 L. Liu, P. Hao, R. Zhang, Y. Zhang, Q. Zhou, X. Lu, D. Yan, Y. Li and C. Shi, *J. Appl. Polym. Sci.*, 2023, **140**, e54238.
- 33 C. Fu, J. Liu, H. Xia and L. Shen, *Prog. Org. Coat.*, 2015, **83**, 19–25.
- 34 F. Yang, H. Yu, Y. Deng and X. Xu, *e-Polymers*, 2021, **21**, 491–499.
- 35 M. Rhein, A. Demharther, B. Felker and M. A. R. Meier, *ACS Appl. Polym. Mater.*, 2022, **4**, 6514–6520.
- 36 P. S. Lee and S. M. Jung, *J. Appl. Polym. Sci.*, 2022, **139**, 52010.
- 37 A. Duval, D. Vidal, A. Sarbu, W. René and L. Avérous, *Mater. Today Chem.*, 2022, **24**, 100793.
- 38 B. Liu and S. Thayumanavan, *J. Am. Chem. Soc.*, 2017, **139**, 2306–2317.
- 39 Y.-S. Jung, S. Lee, J. Park and E.-J. Shin, *Polymers*, 2022, **14**, 4269.
- 40 B.-X. Cheng, W.-C. Gao, X.-M. Ren, X.-Y. Ouyang, Y. Zhao, H. Zhao, W. Wu, C.-X. Huang, Y. Liu, X.-Y. Liu, H.-N. Li and R. K. Y. Li, *Polym. Test.*, 2022, **107**, 107489.
- 41 F. Peng, X. Yang, Y. Zhu and G. Wang, *Polymer*, 2022, **239**, 124429.
- 42 A. Mouren and L. Avérous, *Eur. Polym. J.*, 2023, **197**, 112338.
- 43 H. Wang, Y. Li, H. Zhang, X. Lang, X. Wang, L. Cao and C. Zong, *J. Polym. Sci.*, 2025, **63**, 121–132.
- 44 H. J. Hagemeyer, in *Kirk-Othmer Encyclopedia of Chemical Technology*, John Wiley & Sons, Ltd, 2002.
- 45 J. Ackermann, P. Radici and P. Erini, *United States*, US3911046A, 1975.

